Applying Multiobjective Genetic Algorithm to Analyze the Conflict among Different Water Use Sectors during Drought Period

Liang-Cheng Chang[1]; Chih-Chao Ho[2]; and Yu-Wen Chen[3]

Abstract: Water deficits often occur during the drought season and may cause water conflicts among various water use sectors. The reservoir rule curve operation is commonly used to avoid extreme water shortage during droughts in Taiwan. When applying the rule curve operation, the water supply discounting ratio for different sectors implies a trade-off of water deficit impact among sectors. This study therefore develops a multiobjective water resource management model to evaluate the trade-off curve of water deficit impact between irrigation and public sectors to facilitate negotiation between the sectors for obtaining acceptable discounting ratios. The study uses the shortage index to assess water deficit impact. The proposed model integrates operating rules, the stepwise optimal water allocation model, and the convex hull multiobjective genetic algorithm to solve the multiobjective regional water allocation planning problem. The computed trade-off curve, noninferior solutions, provides relevant information to facilitate negotiating water-demand transfer. The results reveal that when decision makers prefer specified water use, the discounting ratio of another competing water use at the low buffer zone should be limited on the lower bound.

CE Database subject headings: Water management; Droughts; Algorithms; Water use.

Author keywords: Trade-off curve; Stepwise optimal water allocation (SOWA) model; Convex hull multiobjective genetic algorithm (cMOGA).

Introduction

Increasing expense and environmental impact of traditional water resource facilities (e.g., reservoirs) have motivated the requirement of increasing operating efficiency for existing facilities instead of developing new ones (Lund and Israel 1995). During the drought season, system managers would rather incur a sequence of smaller water supply shortages than one potential catastrophic shortage (Lund and Reed 1995). To mitigate the consequences of potential failures, system managers commonly use rule curves to regulate reservoir operation and increase operating efficiency in Taiwan. The rule curve principle is to moderate the current water supply of different water use sectors during drought and retain an adequate amount of water in reservoirs for future use (Tu et al. 2008). When applying rule curve operations, the reservoir volume must be divided into several operating zones and the water supply discounting ratio for different water use sectors is specified for

each zone. The discounting ratio value may differ for distinct water use sectors even at the same operating zone. Determining discounting ratio values implies a water use trade-off among water use sectors and is a water supply conflict issue during drought. Providing quantitative water deficit impact information is therefore important for facilitating negotiation among different water use sectors to obtain acceptable discounting ratios for each sector.

From the system analysis viewpoint, the water conflict problem caused by limited water resources is a multiobjective planning problem. For a typical multiobjective planning problem, the mutually conflicting objectives represent different sector preferences and various objectives may be incommensurable. The weighting method and ε-constraint method are commonly applied for solving a multiobjective planning problem (Cohon and Marks 1977). Conventionally, these methods require transferring the original problem. The weighting method sums the multiple objective functions with weights into a single objective. The ε-constraint method incorporates objectives into the constraint set. After transforming the problem, these methods apply a gradient-based nonlinear programming (NLP) method to solve the problem. A gradient-based NLP method requires differentiability of the objective function and related variables. Since the water supply discounting ratios are noncontinuous when the water level drops into another operating zone, these methods are difficult to apply. To avoid transferring the original problem and overcoming discontinuity induced by the rule curve operation, this study applies the multiobjective genetic algorithm (MOGA) to solve the multiobjective planning problem. MOGA is an attractive approach because it does not require continuous variables and can

[1]Professor, Dept. of Civil Engineering, National Chiao Tung Univ., 1001 Univ. Rd., Hsinchu, Taiwan 300, Republic of China. E-mail: lcchang31938@gmail.com

[2]Ph.D. Candidate, Dept. of Civil Engineering, National Chiao Tung Univ., Hsinchu, Taiwan, Republic of China (corresponding author). E-mail: zz0813@gmail.com

[3]Post-Doctor, Dept. of Civil Engineering, National Chiao Tung Univ., Hsinchu, Taiwan, Republic of China. E-mail: bsjacky@gmail.com

identify convex and nonconvex points on the Pareto frontier (Cieniawski et al. 1995).

Many researches have successfully integrated MOGA with other methods to solve various water resource planning problems. For example, Yeh and Labadie (1997) combined MOGA with successive reaching dynamic programming (SRDP) to solve the planning of a watershed detention dam system in a multiobjective framework and overcome complexity when both location and sizing of detention dams are involved. The basin and channel routing was imbedded in the SRDP. Prasad and Park (2004) integrated MOGA with the hydraulic network solver EPANET to design a water distribution network for minimizing pipe network costs and maximizing reliability. Yang et al. (2007) developed an integration model of MOGA and constrained differential dynamic programming (CDDP) to solve a surface and subsurface conjunctive use problem. The objective is to minimize fixed costs and operating costs and adopt the CDDP to compute optimal releases among reservoirs that fulfill water demand as much as possible. In these studies, computational loading for the integrated model increased greatly with increasing state variable numbers when embedding a DP-based algorithm. Following these hybrid approaches and to reduce computational loading, this study proposes a hybrid model that embeds a stepwise optimal water allocation (SOWA) model into the convex hull multiobjective genetic algorithm (cMOGA) to solve the water distribution problem. cMOGA is the MOGA based algorithm, which follows the study of Feng et al. (1997). SOWA incorporates an optimization scheme [linear programming (LP)] into a simulation framework to compute water supply based on rule curve operation. According to the rule curve operation, target water demand is discontinuous when the reservoir storage level is in different operating zones. The SOWA overcomes discontinuity difficulty resulting from the rule curve operation.

Model Formulation

This study develops the proposed hybrid model by embedding a SOWA model into the cMOGA algorithm. This work aims to minimize irrigation and public sector deficits. These are mutually conflicting objectives during drought because of finite water resources. The study uses the shortage index (SI) to assess the water deficit impact for the two sectors, respectively. The SI, proposed by the U.S. Army Corps of Engineers, is used to surrogate water shortage impact in Taiwan.

For each water use sector, the SI is defined as

$$SI = \frac{100}{N} \sum_{i=1}^{N} \left(\frac{SH_i}{T_i} \right)^2 \tag{1}$$

where N denotes the number of periods; SH_i = water shortage volume during period i; and T_i represents demand of the water use sector (agriculture or industry) during period i. Each period in this research is 10 days, commonly used in Taiwan when performing long-term studies for water resources planning.

These two competing system objectives are expressed as

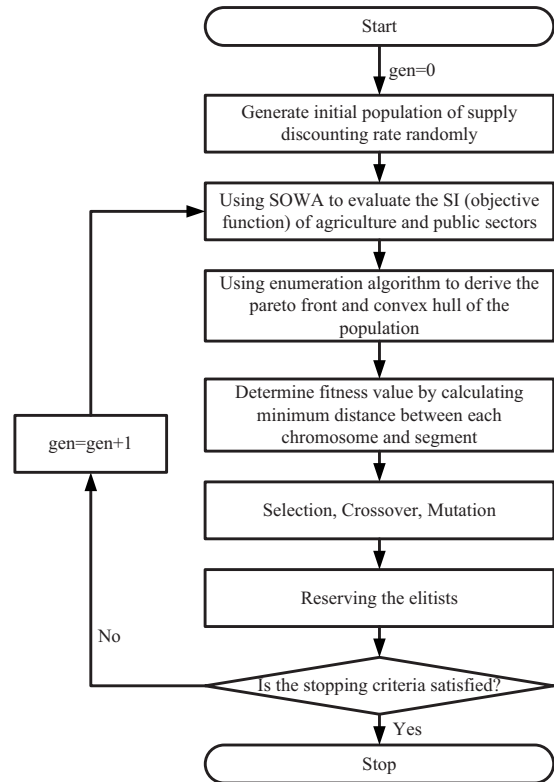$$\vec{J} = \min_{\vec{L}} [SI_1(\vec{L}), SI_2(\vec{L})] \tag{2}$$

subject to


Fig. 1. Flowchart of the cMOGA model

$$SOWA \ model \tag{3}$$

where $SI_1(\vec{L})$ and $SI_2(\vec{L})$ = SIs of agricultural water use and public water use, respectively, and both are to be minimized. $\vec{L}$ is the decision variable (the supply discounting ratios of the rule curve). The complete multiobjective problem is solved based on cMOGA. The SOWA is used to assess the objective function and the decision variables are part of the SOWA inputs. The next section illustrates the detailed description of cMOGA and SOWA.

cMOGA Model

The MOGA based algorithm in this study follows the study of Feng et al. (1997), named as the cMOGA. Fig. 1 shows the main procedure of the cMOGA. The population of supply discounting ratios of agriculture and industry is first randomly generated by a binary code. Then the SIs for the two sectors, respectively, are evaluated for each chromosome by the proposed SOWA model.

This procedure next applies a proposed enumeration algorithm to derive the Pareto front and convex hull of the population (Feng et al. 1997). The Pareto front of the population can be mathematically expressed in terms of noninferior solutions. If Solution S1 is better than S2 in terms of all objective values, Solution S1 dominates S2. If Solution S1 dominates any other solutions in the population, Solution S1 is a noninferior solution. The set of noninferior solutions is the Pareto front of the population. The convex hull denotes a convex boundary composed by a set of linear segments and enclosed by all feasible solutions. Fig. 2 shows the convex hull and the Pareto front. The convex hull is derived from the Pareto front.
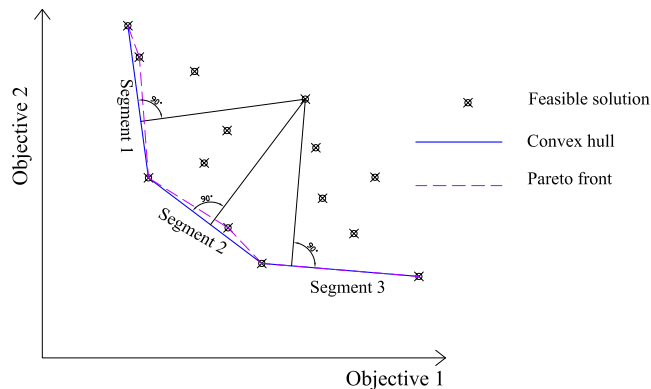
Fig. 2. Trade-off curve, convex hull, and fitness calculation

Based on the study of Feng et al. (1997), fitness for each chromosome equals the shortest distance between the convex hull and the chromosome. The fitness is computed according to

$$f_i = \min(d_{ij}) \tag{4}$$

where f_i=fitness value of the ith chromosome, and d_{ij}=shortest distance between the ith chromosome and the jth segment (Fig. 2).

After defining the fitness value of each chromosome, the next step generates offspring of the generation through selection, crossover, and mutation. Those operations are similar to a conventional simple genetic algorithm. This work applies a tournament method with pairwise fitness comparison for offspring selection, and a chromosome with a lower f_i value has higher priority to be selected as offspring.

To further change offspring attributes, crossover and mutation operations were performed. Furthermore, this study applies the elitism approach to preserve the best solutions through generations and to speed up convergence. The procedure is repeated until achieving convergence. Convergence is the variation ratio (VR) between two generations less then 5% for ten consecutive generations. The VR is defined as

$$VR_{i+1} = \left(1 - \frac{\text{num}(P_{i+1} \cap P_i)}{\text{num}(P_{i+1})}\right) \times 100\% \tag{5}$$

where the subscript i denotes the ith generation; P_i=set of noninferior solutions for the ith generation; num( )=operator to calculate the number of set members; $\cap$=operator of intersection; and VR_{i+1}=variation ratio of the noninferior solution between the ith and $(i+1)$th generations.

SOWA Model

Simulation models (e.g., the HEC-5 model) have been successfully used in water allocation problem. However, recent studies have tended toward incorporating an optimization scheme into the simulation model to perform certain degrees of optimization. (Wei and Hsu 2008). These optimization schemes typically include the DP, LP, or NLP (Yeh and Labadie 1997; Yang et al. 1996; Labadie 2004). Choosing an optimization model depends on the considering system characteristics (Tu et al. 2003). LP has been widely adopted for water allocation systems (Wei and Hsu 2008; Sun et al. 1995; Fredericks et al. 1998).

This study also uses LP to optimally allocate the water to different water-demand sectors. Instead of optimizing globally in
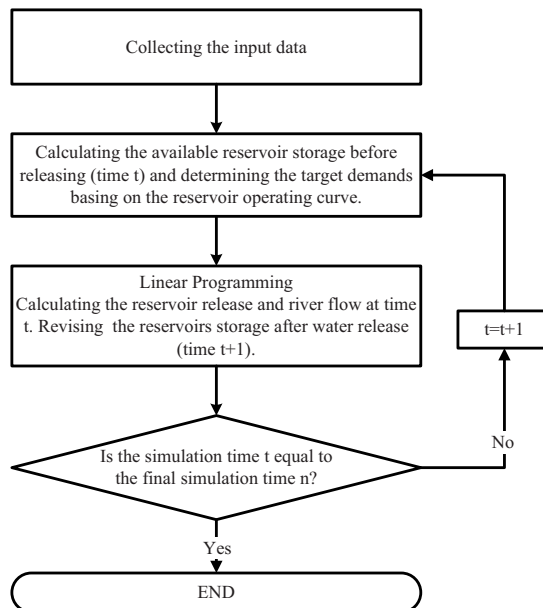
Fig. 3. Flowchart of the SOWA model

time, LP computes the optimal release at each time step for a model called the SOWA model. The model can allocate water to various water-demand sectors (such as agriculture and public sectors), while preserving an in-stream ecological base flow.

Fig. 3 shows the flowchart of the SOWA model. The input data should first be prepared for the simulation model. Those data include the inflow, demand, and capacity of hydraulic facilities, etc., collected from related project reports of the Water Resources Agency in Taiwan. Second, although each water use sector has its required water demand, the water-demand target should be fulfilled at each time step depending on the reservoir operating rules. The reservoir operating rule is applied to determine the target water demand of each water use sector according to the demand discounting ratio and reservoir storage before releasing. Third, based on the proposed formulation (objective function and constraints), this work use linear program is to compute the reservoir releases and the associated river flow at each time step. The reservoir storage is revised after the reservoir releases. The procedure is repeated until the simulation time t is equal to the final time step. The LP model is the major computing routing in the third step. The following illustrates the detailed description of the model.

Objective Function of SOWA

The objective function of the linear model in SOWA at each time step t can be shown as

$$Z^t = \min\left\{\left(\sum_{i \in N_D} W_{SH,i} SH_i^t\right) + \left(\sum_{F \in N_F} W_{G,F} G_F^t\right) + \left(\sum_{j \in N_S} W_{SP,j} X_{SP,j}^t\right)\right\}$$

$$W_{SH,i} > W_{G,F} > W_{SP,J} \tag{6}$$

The first term (SH_i^t) of objective function denotes the water shortage of demand i. Minimizing the demand shortage implies fulfilling the water demand as much as possible. The second term (G_f^t) of the objective function denotes the discrepancy of water-level index among different reservoirs. Minimizing the index discrepancy implements the principle of "balanced water-level index" proposed in the HEC-5 developed by the U.S. Army Corps of

Engineers. The formulary definition of G_f^t is defined in constraint (8). The last term ($X_{SP,j}^t$) of the objective function is the remaining reservoir vacancy. Minimizing vacancy is storing the water in reservoirs as much as possible. The weighting parameters $W_{SH,i}$, $W_{G,F}$, and $W_{SP,J}$ represent the priorities of their associated objectives; the higher the values, the greater the objective importance.

Constraints of SOWA

Continuity Equations

$$S_i^{t+1} = S_i^t + \sum I_i^t - E_i^t - \sum X_i^t - OF_i^t$$

$$\forall i \in N_s \qquad (7)$$

Eq. (7) is the continuity equation for reservoir water storage, where S_i^{t+1} and S_i^t denote the storages of reservoir i at t and $t+1$ time step, respectively; I_i^t, E_i^t, X_i^t, and OF_i^t are the inflow, evaporation, outflow, and overflow for reservoir i at time step t, respectively; and N_s is the set of all reservoirs. The continuity equations for other system nodes such as weirs and river conjunctions are similar to Eq. (7) but the S_i^{t+1}, S_i^t, and OF_i^t equal to zero.

Institutional Constraints

$$\frac{S_i^t - \Sigma_{k \in N_i} X_{i,k}^t - LAY_{i,n}^t}{LAY_{i,(n+1)}^t - LAY_{i,n}^t} + G_F^t = \frac{S_j^t - \Sigma_{l \in N_j} X_{j,l}^t - LAY_{j,n}^t}{LAY_{j,(n+1)}^t - LAY_{j,n}^t}$$

$$\forall i, \quad j \in N_S, \quad \forall k \in N_i, \quad \forall l \in N_j, \quad \forall F \in N_F \qquad (8)$$

where G_F^t denotes the discrepancy of water-level index among different reservoirs at time step t; $X_{i,k}^t(X_{j,l}^t)$ denotes the outflow withdrawing from reservoir $i(j)$ to demand $k(l)$ at time step t; $LAY_{i,n}^t$ ($LAY_{j,n}^t$) indicates the nth operation zone of reservoir $i(j)$ at time step t; $LAY_{i,(n+1)}^t$ ($LAY_{j,(n+1)}^t$) indicates the $(n+1)$th operation zone of reservoir $i(j)$; N_i = set of all demands that were supplied by reservoir i; and N_j = set of all demands that are supplied by reservoir j. Eq. (8) refers to the principle of balance water-level index for increasing the long-term water allocation performance for a multireservoir system. The balance water-level index method is an extension of rule curve operation for a single reservoir and each reservoir has to divide its volume into several operational zones before applying the method.

Ecological Base Flow Constraint

$$R_{i,j}^t \geq \min\left(\sum_{m \in \Pi_{i,j}} I_m^t, B_{i,j}^t \right) \qquad (9)$$

Eq. (9) represented the constraint of in-stream ecological base flow that needs to be fulfilled at each time step, where $R_{i,j}^t$ = ecological base flow to be fulfilled in river section (i,j) at time step t; I_m^t = mth inflow upstream of river section (i,j); and $B_{i,j}^t$ = ecological base flow demand. The value of $B_{k,t}$ is equal to Q_{95}, which means the river flow has 95% of the opportunities greater than discharge Q_{95}. $\Pi_{i,j}$ denotes the set of all inflows upstream of river section (i,j). Eq. (9) indicates that the ecological base flow demand will be fulfilled if there is enough upstream inflow for the river section. Otherwise, the base flow will be the summation of the upstream inflows.

Water Balance at Demand Node

$$D_j^t = \sum_{i \in \Lambda} X_{i,j}^t + SH_j^t, \quad \forall j \in N_D \qquad (10)$$

where D_j^t = target demand of demand node j at time step t; $X_{i,j}^t$ denotes the outflow withdrawing from node i and supply to demand j at time step t; SH_j^t = water shortage of demand node j; N_D denotes the set of all demand nodes; and Λ indicates the set of all outflows that supply to node j.

Capacity Constraints

Capacity constraints define the capacity of reservoir storage, channels, pipes, and water treatment plant. The reservoir storage ranges from full capacity ($S_{u,i}$) to dead storage ($S_{d,i}$) over the planning horizon and can be represented as follows:

$$S_{d,i} \leq S_i^t \leq S_{u,i}, \quad \forall i \in N_S \qquad (11)$$

The water supply is subjected to the pipe capacity, and can be represented as

$$0 \leq X_i^t \leq P_i^t, \quad \forall i \in N_P \qquad (12)$$

where X_i^t denotes the pipe flow i at time step t; P_i^t = pipe capacity i at time step t; and N_P = set of all pipes.

Moreover, the water supply is also subjected to the capacity of water treatment plant, and can be represented as

$$0 \leq \sum_{j \in NU_i} X_{i,j}^t \leq U_j^t \qquad (13)$$

where $X_{i,j}^t$ denotes the water supply to demand j from water treatment plant i at time step t; U_j^t = capacity of water treatment plant j at time t; and NU_i = set of demands supplied from water treatment plant i.

Case Study

This study applies a hybrid model to manage and operate a complex real-world multireservoir system. The study region covers two metropolitan areas, Tainan and Kaoshing, and part of ChiaYi County in Southern Taiwan. Fig. 4 shows the water distribution system. The main water sources derive from the Nan-Hua Reservoir, the Tseng-Wen Reservoir, the Wu-Shan-Tou Reservoir, and the Kaopin-Hsi Weir. Among these facilities, the Kaopin-Hsi Weir is located downstream from the KaoPin River and the others are situated in the Tseng-Wen river basin. The Nan-Hua Reservoir draws KaoPin river basin water through the Tung-Kou Weir. Four main existing water treatment plants and one planning water treatment plant are located in Southern Taiwan: the Pin-Tin water treatment plant, the Nan-Hua water treatment plant, the Wu-Shan-Tou water treatment plant, the Tan-Tin water treatment plant, and the Feng-Chuang water treatment plant, respectively. The basic water distribution principle is to use water from the Kaopin-Hsi Weir first, then from the other three reservoirs.

The other operating rule is to sequentially fulfill the demands depending on the water source withdrawn. For water withdrawn from the Kaopin River, the Kaoshing public use demand has higher priority over the Tainan public use demand; for water withdrawn from three reservoirs, the water supply priority is to meet the Wu-Shan-Tou irrigation demand, the Tainan public use demand, and the Kaoshing public use demand in sequence. The public use demand includes water for domestic and industrial uses. The three reservoirs operate together as a multireservoir
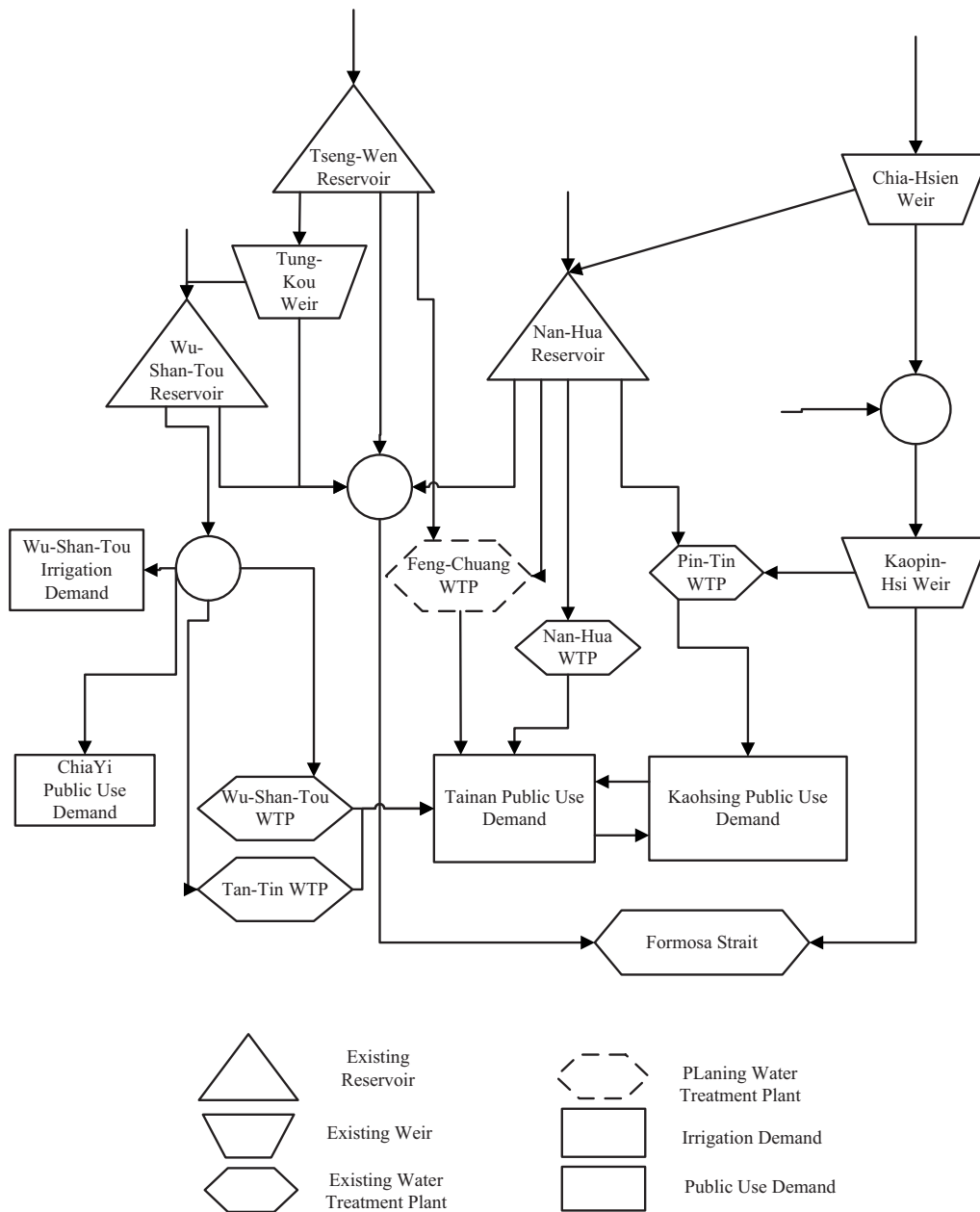
**Fig. 4.** Water distribution system of the study area

system, and the amount of water released from each reservoir is managed according to the balanced water-level index provided by the U.S. Army Corps of Engineers.

Reservoir operation should also be based on the operating curve of an equivalent reservoir. The operating curve is based on the equivalent reservoir combined with the Tseng-Wen Reservoir and the Wu-Shan-Tou Reservoir. The operating curve varies by months according to the changes in meteorological and hydrologic conditions (Fig. 5). The operating curve divides equivalent reservoir volume into four operating zones; they are low buffer zone, high buffer zone, conservation zone, and flood control zone. Each zone has different criteria for decreasing target demand, depending on how much water has been stored in the equivalent reservoir.

This study includes four decision variables, which are the weightings (supply discounting ratio) at high buffer zone and low buffer zone for agriculture and public use. The decision variables
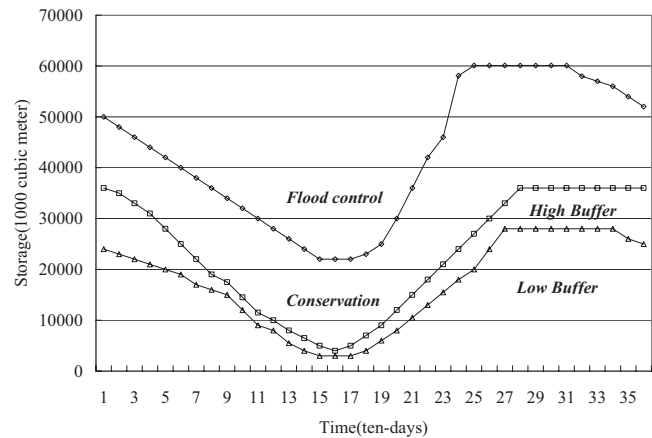
Fig. 5. Definition of the reservoir operating zone for the equivalent reservoir of Tseng-Wen Reservoir and Wu-Shan-Tou Reservoir
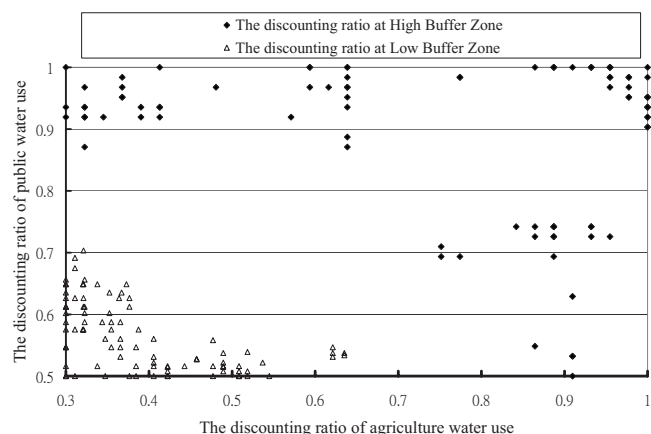
JOURNAL OF WATER RESOURCES PLANNING AND MANAGEMENT © ASCE / SEPTEMBER/OCTOBER 2010 / **543**
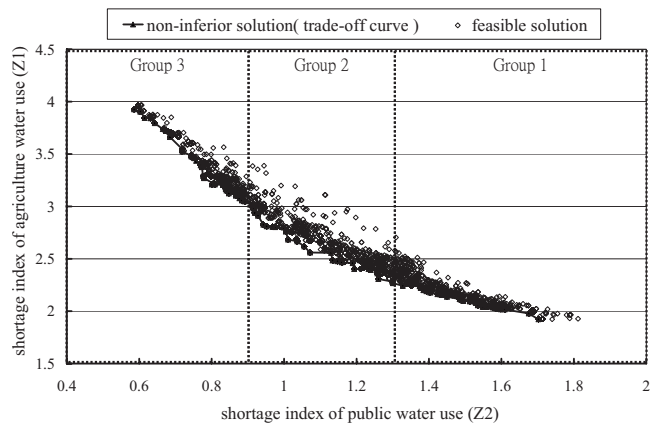
Fig. 6. Trade-off curve between the SI of agriculture water and that of public water (final population)

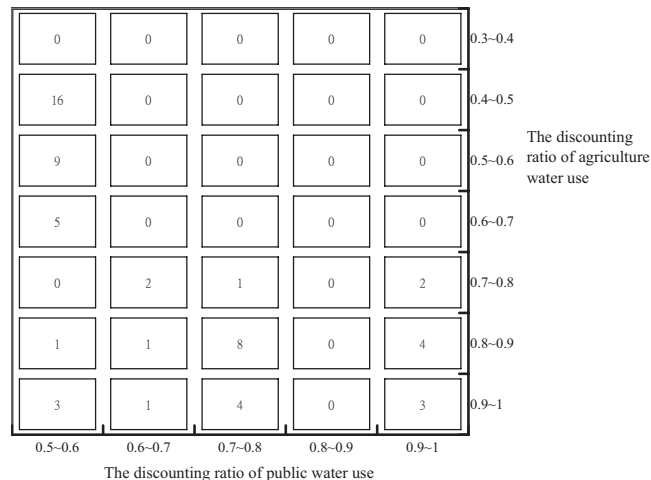**Fig. 8.** Occurrence frequency distribution of discounting ratios for the first group

must be coded as chromosomes and each decision variable is coded as eight binary bits. Because the agriculture and public sector have different degrees of enduring deficit abilities, the weighting range should be set differently. The weighting range of agriculture use is set from 0.3 to 1 in this study and the weighting range of public use is set from 0.5 to 1. The weighting at the high buffer zone should be larger than the weighting at the low buffer zone. Hence the weighting range at the low buffer zone for agriculture and public use should be revised as from 0.3 to the agriculture weighting value of the high buffer zone and from 0.5 to the public weighting value of the high buffer zone, respectively.

Results and Discussion

Fig. 6 presents the trade-off curve for the SI of agriculture water use (Z1) and SI of public water use (Z2) computed by cMOGA. The noninferior solutions were obtained after 208 generations with a population size of 200, and the convergence criterion is that VR is less then 5% for ten consecutive generations (Fig. 7). Fig. 6 indicates that the minimum SI of agriculture water use is approximately 1.98 when the maximum SI of public water use is 1.70. On the other hand, the maximum SI of agriculture water use is 3.93 when the minimum SI of public water use is approximately 0.59. For all noninferior solutions, the SI of agriculture water is always higher than that of public water. This situation is

caused because agriculture water can only be supplied by the Tseng-Wen Reservoir and the Wu-Shan-Tou Reservoir but the public use water has other water sources, the Kaopin-Hsi Weir, the Chia-Hsien Weir, and the Nan-Hua Reservoir (refer to Fig. 4).

Fig. 7 displays the distribution of decision variables' value for noninferior solutions to explore their structure. Each feasible solution has four decision variables, the discounting ratios for agriculture and public water use at the high buffer zone ($C_{1,1}$ and $C_{2,1}$) and those at the low buffer zone ($C_{1,2}$ and $C_{2,2}$). The first suffix of variables denotes water use type and the second suffix represents different buffer zones. Fig. 7 clearly shows that the distribution of discounting ratios for the two buffer zones is separated into two groups. As expected, the low buffer zone distribution is enclosed by the distribution at the high buffer zone. The discounting ratios for the low buffer zone clusters near the lower left corner with $C_{1,2}$ range roughly between 0.3 and 0.7, and $C_{2,2}$ range roughly between 0.5 and 0.65. The discounting ratios for the high buffer zone distribute are much more scattered than those of the low buffer zone, which is discussed further in the following.

The study divides the noninferior solutions into three groups, depending on the objective values (Fig. 6) to analyze the relationship among objectives and decision variables. The first group emphasizes the agriculture water demand; therefore, it has the higher end of the range for the public SI (1.328–1.702) and the lower end of the range for agriculture SI (1.978–2.242). The second group equally emphasizes the public and agriculture water demands, and the SI value ranges are 0.884–1.328 and 2.242–3.057, respectively. The third group emphasizes the public water demand; thus, it has the lower end of the range for the public SI (0.586–0.884) and the higher end of the range for the agriculture SI (3.057–3.927).

Figs. 8–10 show the occurrence frequency for discounting ratios of agriculture and public water use with respect to different groups. A higher value of discounting ratio indicates a higher priority for fulfilling the associated water demand. For the high buffer zone and the low buffer zone, the discounting ratios of agriculture for the first group (Fig. 8) concentrate on higher value than those for the third group (Fig. 10). The discounting ratios of public water demand for the first group are expected to concentrate on the lower value than that for the third group. However, the result is not as clear as that for agriculture. For the low buffer

Fig. 7. Distribution of discounting ratios for the two buffer zones

The discounting ratio of agriculture water use	0.5~0.6	0.6~0.7	0.7~0.8	0.8~0.9	0.9~1
0.3~0.4	16	9	0	0	0
0.4~0.5	5	0	0	0	0
0.5~0.6	0	0	0	0	3
0.6~0.7	0	0	0	0	2
0.7~0.8	0	0	0	0	0
0.8~0.9	0	0	0	0	0
0.9~1	0	0	0	0	25

The discounting ratio of public water use
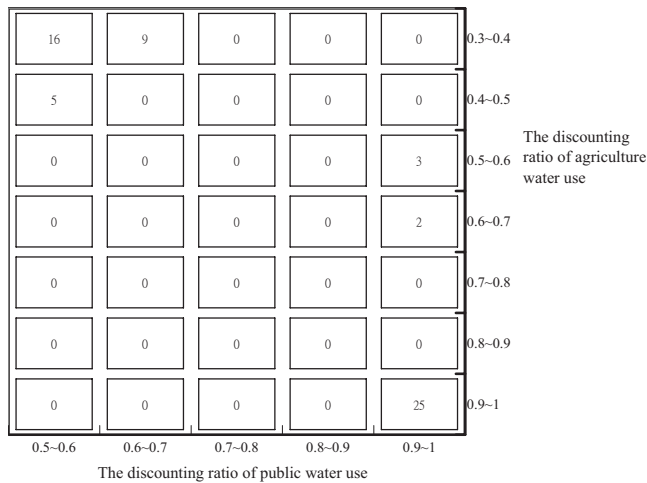
Fig. 9. Occurrence frequency distribution of discounting ratios for the second group

zone, as expected, $C_{2,2}$ for the first group concentrates more on the lower value than that of the third group. Nevertheless, for the high buffer zone, although $C_{2,1}$ for the third group still concentrates on high value as expected (Fig. 10), $C_{2,1}$ for the first group does not concentrate on low value but varies widely in the feasible range (0.5–1) (Fig. 8).

The water supply system structure shown in Fig. 4 explores the exception for $C_{2,1}$ when emphasizing agriculture water demand. Fig. 4 indicates that only two reservoirs (Tseng-Wen Reservoir and Wu-Shan-Tou Reservoir) supply the agriculture demand (Wu-Shain-Tou irrigation demand), while the public water demands (Tainan and Kaoshing, and part of ChiaYi County public demand) can be supplied by all five major water sources (Tseng-Wen, Wu-Shan-Tou, Nan-Hua Reservoir, and Kaopin-Hsi, Chia-Hsien Weir). The system structure induces that, when water level is in the high buffer zone, the public demands withdraw from their independent water sources (Kaopin-Hsi Weir, Chia-Hsien Weir, and Nan-Hua Reservoir) and do not struggle for the water stored in Tseng-Wen and Wu-Shan-Tou Reservoirs with the agriculture demand. This does not force the discounting ratio of public water demand to low value and induces the discounting

The discounting ratio of agriculture water use	0.5~0.6	0.6~0.7	0.7~0.8	0.8~0.9	0.9~1
0.3~0.4	12	17	1	1	15
0.4~0.5	0	0	0	0	5
0.5~0.6	0	0	0	0	1
0.6~0.7	0	0	0	2	6
0.7~0.8	0	0	0	0	0
0.8~0.9	0	0	0	0	0
0.9~1	0	0	0	0	0

The discounting ratio of public water use
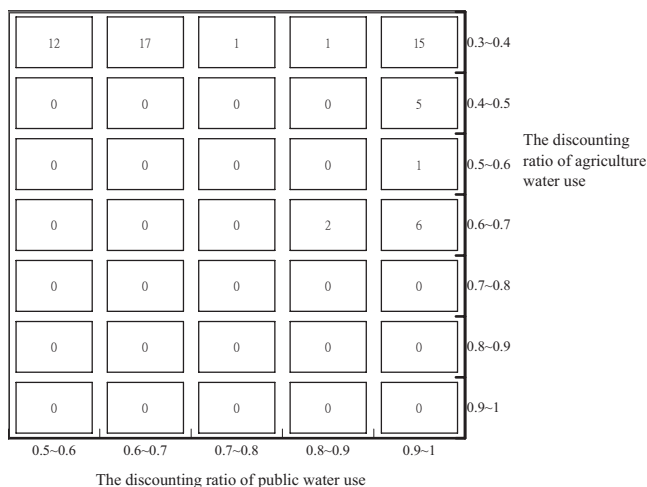
Fig. 10. Occurrence frequency distribution of discounting ratios for the third group

ratio of public water demand to vary widely in its feasible region even with emphasizing agriculture demand (shown as Fig. 8). However, when the water level drops in the low buffer zone in severe dry season, with supplying less water to the public demand from Kaopin-Hsi Weir, Chia-Hsien Weir, and Nan-Hua Reservoir, it will induce public water use and agriculture water use to struggle for the limited water stored in the Tseng-Wen and Wu-Shan-Tou Reservoirs. Hence, emphasizing agriculture water demand forces the discounting ratio of public water demand to low value (shown as Fig. 8).

Fig. 9 indicates that, when equally emphasizing agriculture and public demand, the discounting ratios for both water demands vary in the same trend. The high buffer zone trend slightly restricts the water-demand supply (both $C_{1,1}$ and $C_{2,1}$ range between 0.9 and 0.1). the low buffer zone trend severely restricts the water-demand supply ($C_{1,2}$ ranges between 0.3 and 0.4 and $C_{2,2}$ ranges between 0.5 and 0.6).

Conclusions

To overcome the limitations of using conventional multiobjective optimization methods to solve water sharing conflict problems, this paper develops a novel multiobjective hybrid model that integrates a cMOGA with a rule curve based reservoir operation model (SOWA). The study applies the proposed model to solve the conflict between different water use sectors. The proposed hybrid model generates different alternatives in a single run, increasing the efficiency of obtaining noninferior solutions (trade-off curve). The case study demonstrates that the proposed model solves a practical multiobjective water resource planning problem. The discounting ratios of noninferior solutions provide relevant information to facilitate stakeholders negotiating under different preferences. The results also reveal how the decision makers' preference influences the discounting ratios of difference water use. When decision makers prefer agriculture use to public use, the discounting ratio of public use at the low buffer zone should be limited on the lower bound. The discounting ratio of agriculture use at the low buffer zone should, however, be limited on the lower bound when decision makers prefer public use to agriculture use. Without particular preference, the discounting ratios of agriculture use and public use at the low buffer zone both should be limited on the lower bound. Therefore, stakeholder preference is also an important factor for a multiobjective water resource allocation problem.

References

Cieniawski, S. E., Eheart, J. W., and Ranjithan, S. (1995). "Using genetic algorithms to solve a multiobjective groundwater monitoring problem." *Water Resour. Res.*, 31, 399–409.

Cohon, J. L., and Marks, D. H. (1977). "Review and evaluation of multiobjective programming techniques—Reply." *Water Resour. Res.*, 13, 693–694.

Feng, C. W., Liu, L. A., and Burns, S. A. (1997). "Using genetic algorithms to solve construction time-cost trade-off problems." *J. Comput. Civ. Eng.*, 11(3), 184–189.

Fredericks, J. W., Labadie, J. W., and Altenhofen, J. M. (1998). "Decision support system for conjunctive stream-aquifer management." *J. Water Resour. Plann. Manage.*, 124(2), 69–78.

Labadie, J. W. (2004). "Optimal operation of multireservoir systems: State-of-the-art review." *J. Water Resour. Plann. Manage.*, 130(2), 93–111.

Lund, J. R., and Israel, M. (1995). "Water transfers in water-resource systems." *J. Water Resour. Plann. Manage.*, 121(2), 193–204.

Lund, J. R., and Reed, R. U. (1995). "Drought water rationing and transferable rations." *J. Water Resour. Plann. Manage.*, 121(6), 429–437.

Prasad, T. D., and Park, N. S. (2004). "Multiobjective genetic algorithms for design of water distribution networks." *J. Water Resour. Plann. Manage.*, 130(1), 73–82.

Sun, Y. H., Yeh, W. W. G., Hsu, N. S., and Louie, P. W. F. (1995). "Generalized network algorithm for water-supply-system optimization." *J. Water Resour. Plann. Manage.*, 121(5), 392–398.

Tu, M. Y., Hsu, N. S., Tsai, F. T. C., and Yeh, W. W. G. (2008). "Optimization of hedging rules for reservoir operations." *J. Water Resour. Plann. Manage.*, 134(3), 3–13.

Tu, M. Y., Hsu, N. S., and Yeh, W. W. G. (2003). "Optimization of reservoir management and operation with hedging rules." *J. Water Resour. Plann. Manage.*, 129(2), 86–97.

Wei, C., and Hsu, N. (2008). "Multireservoir real-time operations for flood control using balanced water level index method." *J. Environ. Manage.*, 88, 1624–1639.

Yang, C., Chang, L., Yeh, C., and Chen, C. (2007). "Multiobjective planning of surface water resources by multiobjective genetic algorithm with constrained differential dynamic programming." *J. Water Resour. Plann. Manage.*, 133(6), 499–508.

Yang, S. L., Hsu, N. S., Louie, P. W. F., and Yeh, W. W. G. (1996). "Water distribution network reliability: Stochastic simulation." *J. Infrastruct. Syst.*, 2(2), 65–72.

Yeh, C. H., and Labadie, J. W. (1997). "Multiobjective watershed-level, planning of storm water detention systems." *J. Water Resour. Plann. Manage.*, 123(6), 336–343.

546 / JOURNAL OF WATER RESOURCES PLANNING AND MANAGEMENT © ASCE / SEPTEMBER/OCTOBER 2010

J. Water Resour. Plann. Manage. 2010.136:539-546.